

Scaling of anisotropy flows in intermediate energy heavy ion collisions

Y. G. Ma*, T. Z. Yan, X. Z. Cai, J. G. Chen, D. Q. Fang, W. Guo, G. H. Liu, C. W. Ma, E. J. Ma, W. Q. Shen, Y. Shi, Q. M. Su, W. D. Tian, H. W. Wang, K. Wang ^a

^aShanghai Institute of Applied Physics, Chinese Academy of Sciences, P. O. Box 800-204, Shanghai 201800, China

Anisotropic flows (v_1 , v_2 and v_4) of light nuclear clusters are studied by a nucleonic transport model in intermediate energy heavy ion collisions. The number-of-nucleon scalings of the directed flow (v_1) and elliptic flow (v_2) are demonstrated for light nuclear clusters. Moreover, the ratios of v_4/v_2^2 of nuclear clusters show a constant value of 1/2 regardless of the transverse momentum. The above phenomena can be understood by the coalescence mechanism in nucleonic level and are worthy to be explored in experiments.

1. Introduction

Anisotropic flow can reflect the initial state of the heavy ion reaction and evolution dynamics. In addition, the information of the nuclear equation of state (EOS) could be also learned from the flow studies [1, 2, 3, 4, 5, 6, 7, 8, 9, 10, 11]. Many studies of the 1-th and 2-nd anisotropic flows, namely the directed flow and elliptic flow revealed much rich physics in heavy ion collision (HIC) dynamics. Recently, it was demonstrated that the number of constituent-quark (NCQ) scaling exhibits from the measurement of transverse momentum dependence of the elliptic flow for different mesons and baryons in ultra-relativistic Au + Au collision experiments at the Relativistic Heavy Ion Collider (RHIC) in Brookhaven National Laboratory [12], it indicates that the partonic degree of the freedom plays a dominant role in the formation of the dense matter during early stage of collisions. The coalescence or recombination models of the constituent quarks have been proposed to interpret the NCQ-scaling of hadrons at RHIC [13, 14, 15, 16, 17, 18]. On the other hand, the coalescence mechanism has been also used to explain the formation of light fragments and their spectra of kinetic energy or momentum in intermediate energy heavy ion collisions some times ago [19, 20, 21, 22, 23]. In addition, mass dependence of the directed flow was experimentally investigated in a few studies [24, 25]. However, systematic theoretical studies on the anisotropic flow of different nuclear fragments in intermediate energy domain in terms of the coalescence mechanism is still rare.

In this paper, we will investigate the flow scaling of light nuclear fragments in a framework of a nucleonic transport model, namely isospin-dependent quantum molecular dynamics (IDQMD) at intermediate energies. A naive coalescence mechanism in nucleonic level was applied to analyze the fragment flows. Dependences of the number-of-nucleon (NN) of the anisotropic flows, v_1 and v_2 , are surveyed, and the ratio of v_4 to v_2^2 is studied.

*E-mail: ygma@sinap.ac.cn

2. Definition of anisotropic flow and Model Introduction

2.1. Definition of anisotropic flow

Anisotropic flow is defined as the different n -th harmonic coefficient v_n of an azimuthal Fourier expansion of the particle invariant distribution [2]

$$\frac{dN}{d\phi} \propto 1 + 2 \sum_{n=1}^{\infty} v_n \cos(n\phi), \quad (1)$$

where ϕ is the azimuthal angle between the transverse momentum of the particle and the reaction plane. Note that in the coordinate system the z -axis along the beam axis, and the impact parameter axis is labelled as x -axis.

The first harmonic coefficient v_1 represents the directed flow,

$$v_1 = \langle \cos\phi \rangle = \left\langle \frac{p_x}{p_t} \right\rangle, \quad (2)$$

where $p_t = \sqrt{p_x^2 + p_y^2}$ is transverse momentum. v_2 represents the elliptic flow which characterizes the eccentricity of the particle distribution in momentum space,

$$v_2 = \langle \cos(2\phi) \rangle = \left\langle \frac{p_x^2 - p_y^2}{p_t^2} \right\rangle, \quad (3)$$

and v_4 represents the 4-th momentum anisotropy,

$$v_4 = \left\langle \frac{p_x^4 - 6p_x^2 p_y^2 + p_y^4}{p_t^4} \right\rangle. \quad (4)$$

In this work, we will study the above flow components.

2.2. Nucleonic transport model: QMD Model

The Quantum Molecular Dynamics (QMD) approach is an n -body theory to describe heavy ion reactions from intermediate energy to 2 A GeV. It includes several important parts: the initialization of the target and the projectile nucleons, the propagation of nucleons in the effective potential, the collisions between the nucleons, the Pauli blocking effect and the numerical tests. A general review about QMD model can be found in [26]. The IDQMD model is based on QMD model affiliating the isospin factors, which includes the mean field, two-body nucleon-nucleon (NN) collisions and Pauli blocking [27, 28, 29].

In the QMD model each nucleon is represented by a Gaussian wave packet with a width \sqrt{L} (here $L = 2.16 \text{ fm}^2$) centered around the mean position $\vec{r}_i(t)$ and the mean momentum $\vec{p}_i(t)$,

$$\psi_i(\vec{r}, t) = \frac{1}{(2\pi L)^{3/4}} \exp\left[-\frac{(\vec{r} - \vec{r}_i(t))^2}{4L}\right] \exp\left[-\frac{i\vec{r} \cdot \vec{p}_i(t)}{\hbar}\right]. \quad (5)$$

The nucleons interact via nuclear mean field and nucleon-nucleon collision. The nuclear mean field can be parameterized by

$$U(\rho, \tau_z) = \alpha \left(\frac{\rho}{\rho_0}\right) + \beta \left(\frac{\rho}{\rho_0}\right)^\gamma + \frac{1}{2}(1 - \tau_z)V_c + C_{sym} \frac{(\rho_n - \rho_p)}{\rho_0} \tau_z + U^{Yuk} \quad (6)$$

with ρ_0 the normal nuclear matter density (0.16 fm^{-3} is used here). ρ , ρ_n and ρ_p are the total, neutron and proton densities, respectively. τ_z is z th component of the isospin degree of freedom, which equals 1 or -1 for neutrons or protons, respectively. The coefficients α , β and γ are parameters for nuclear equation of state. Two set parameters are used: $\alpha = -124 \text{ MeV}$, $\beta = 70.5 \text{ MeV}$ and $\gamma = 2.0$ which corresponds to the so-called hard EOS, with an incompressibility of $K = 380 \text{ MeV}$; and $\alpha = -356 \text{ MeV}$, $\beta = 303 \text{ MeV}$ and $\gamma = 7/6$ which corresponds to the so-called soft EOS with an incompressibility of $K = 200 \text{ MeV}$; C_{sym} is the symmetry energy strength due to the difference of neutron and proton [26], here $C_{sym} = 32 \text{ MeV}$ is used to consider isospin effects, or $C_{sym} = 0$ for no isospin effect. V_c is the Coulomb potential, U^{Yuk} is Yukawa (surface) potential. In this model, the isospin effects can be included in some terms, such as in-medium nucleon-nucleon cross section and Pauli blocking [27, 28].

The time evolution of the colliding system is given by the generalized variational principal. Since the QMD can naturally describe the fluctuation and correlation, we can study the nuclear clusters in the model [26, 27, 28, 29]. In QMD model, nuclear clusters are usually recognized by a simple coalescence model: i.e. nucleons are considered to be part of a cluster if in the end at least one other nucleon is closer than $\Delta r_{min} \leq 3.5 \text{ fm}$ in coordinate space and $\Delta p_{min} \leq 300 \text{ MeV}/c$ in momentum space [26]. This mechanism has been extensively applied in transport theory for the cluster formation.

3. Number-of-Nucleon Scaling of the Directed and Elliptic Flows

Reactions of $^{40}\text{Ca} + ^{40}\text{Ca}$, $^{86}\text{Kr} + ^{58}\text{Ni}$ and $^{86}\text{Kr} + ^{124}\text{Sn}$ at 25 MeV/nucleon have been simulated by IDQMD. To compare the results from different reactions, the similar centrality has been chosen for the above systems, namely 4-8 fm, 6-10 fm and 7 - 11 fm, respectively. Since the reaction systems tend to freeze-out around 120 fm/c in the model calculation, the physics results can be extracted in the freeze-out stage. In this work, the results are extracted at 200 fm/c. Some parts of physics results have been reported in our recent papers [30, 31].

The directed flow v_1 as a function of rapidity (y) for the above systems has been studied. Fig. 1 shows v_1 versus rapidity (upper panels) and the nucleon-number scaled v_1/A as a function of rapidity. From this figure, we found that the slope of the directed flow as a function of rapidity is negative for three systems at 25 MeV/nucleon, which indicates that attractive mean field is important in such a low energy [10]. Before the nucleon-number scaling, the values of directed flow are different for different-mass clusters: the heavier the clusters, the large the absolute value of directed flow. However, all the curves of rapidity-dependent v_1 almost collapse onto the same curves by dividing v_1 by its number of nucleon, which illustrates that the directed flow of the light nuclear clusters satisfies the number-of-nucleon scaling. Actually, the previous experimental data for light nuclear clusters up to $A = 4$ for $^{86}\text{Kr} + ^{197}\text{Au}$ showed that the directed flow is approximately proportional to mass number [24].

The upper panels of Fig. 2 show transverse momentum dependence of elliptic flow for mid-rapidity light fragments in three calculation cases: hard EOS without isospin related terms (hard_niso), soft EOS with isospin related terms (soft_iso), and soft EOS without isospin related terms (soft_niso). From the figure, it shows that elliptic flows are positive

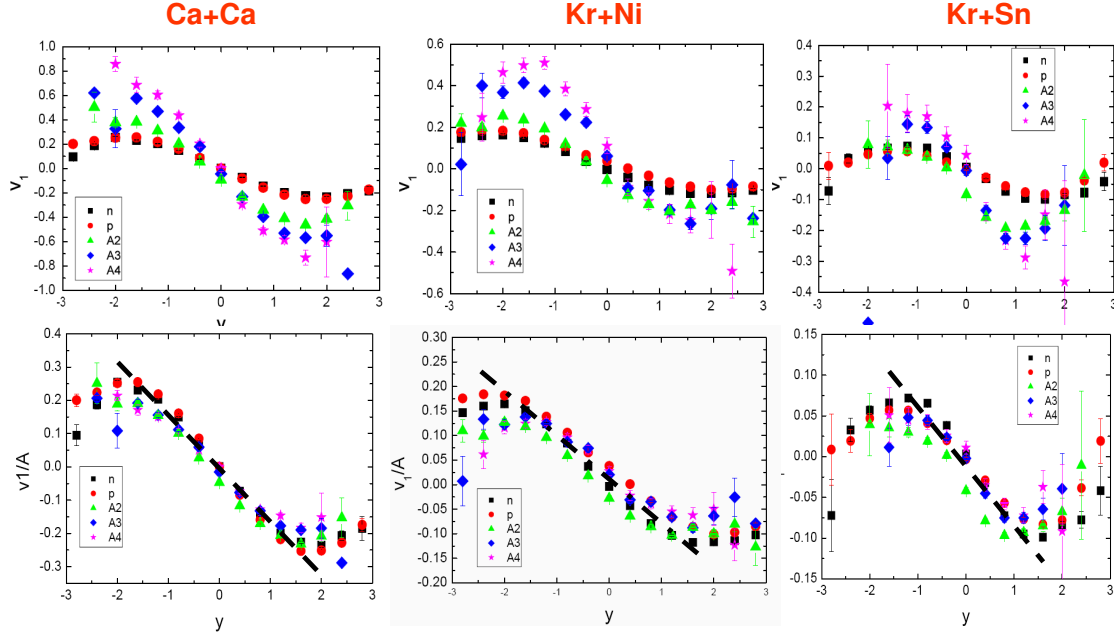


Figure 1. Ca+Ca at 4-8 fm (left panels), Kr + Ni at 6-10 fm (middle panels), Kr + Sn at 7 - 10 fm (right panels). The upper panels show v_1 versus rapidity and the lower panels show v_1/A , i.e. the number-of-nucleon scaled directed flow, versus rapidity. The dashed line guides the eyes.

and increase with the increasing of p_t even though the values are a little different for the different cases. The positive value of v_2 reflects that the light clusters are preferentially emitted within the reaction plane, and particles with higher transverse momentum tend to be strongly emitted within in-plane, i.e. stronger positive elliptic flow. In comparison to the elliptic flow at RHIC energies, the apparent behavior of elliptic flow versus p_t looks similar, but the mechanism is obviously different. In intermediate energy domain, collective rotation is one of the main mechanisms to induce the positive elliptic flow [10, 32, 33, 34, 35, 36]. In this case, the elliptic flow is mainly driven by the attractive mean field. However, the strong pressure which is built in early initial geometrical almond-type anisotropy due to the overlap zone between both colliding nuclei in coordinate space will rapidly transforms into the azimuthal anisotropy in momentum space at RHIC energies [12]. In other words, the elliptic flow is mainly driven by the stronger outward pressure. The lower panels in Fig. 2 displays the elliptic flow per nucleon as a function of transverse momentum per nucleon, and it looks that there exists the number-of-nucleon scaling when $p_t/A < 0.25$ GeV/c. This behavior is apparently similar to the number-of-constituent-quarks scaling of elliptic flow versus transverse momentum per constituent quark (p_t/n) for mesons and baryons which was observed at RHIC [12].

4. v_4/v_2^2 -scaling

Recent the RHIC results show that v_4/v_2^2 for hadrons keeps an almost constant which is independent on p_t [37], we would like to know what the higher order momentum

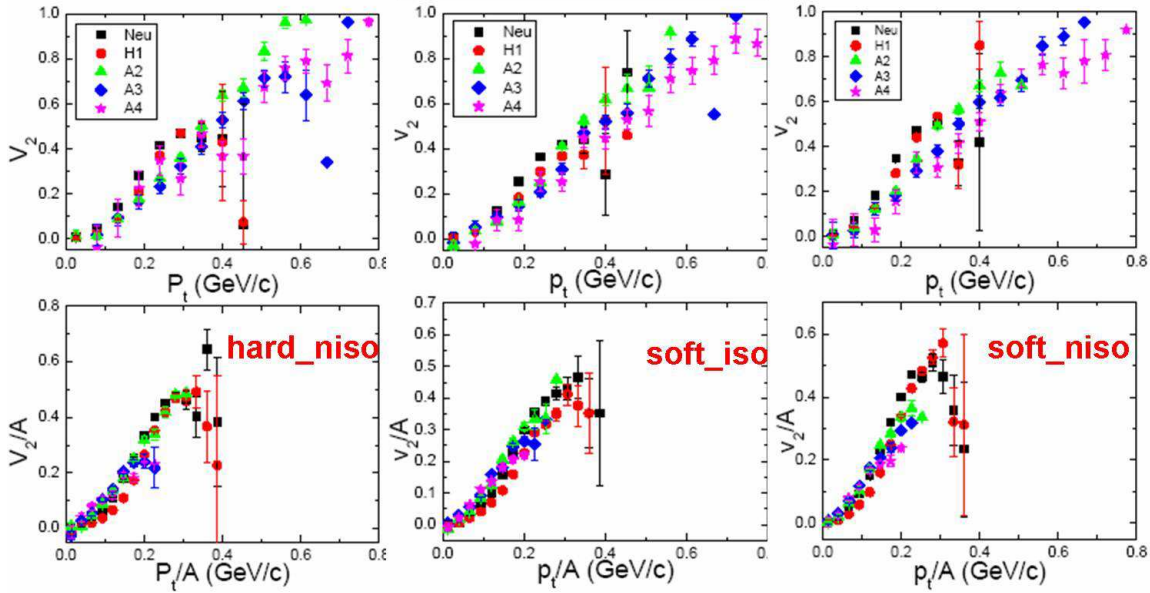


Figure 2. The upper panels: Elliptic flow as a function of transverse momentum (p_t) for $^{86}\text{Kr} + ^{124}\text{Sn}$ at 25 MeV/nucleon. Three simulations were done: hard EOS without isospin related terms (hard_niso), soft EOS with isospin related terms (soft_iso), and soft EOS without isospin related terms (soft_niso). Squares represent for neutrons, circles for protons, triangles for fragments of $A = 2$, diamonds for $A = 3$ and stars for $A = 4$; The lower panels: Elliptic flow per nucleon as a function of transverse momentum per nucleon.

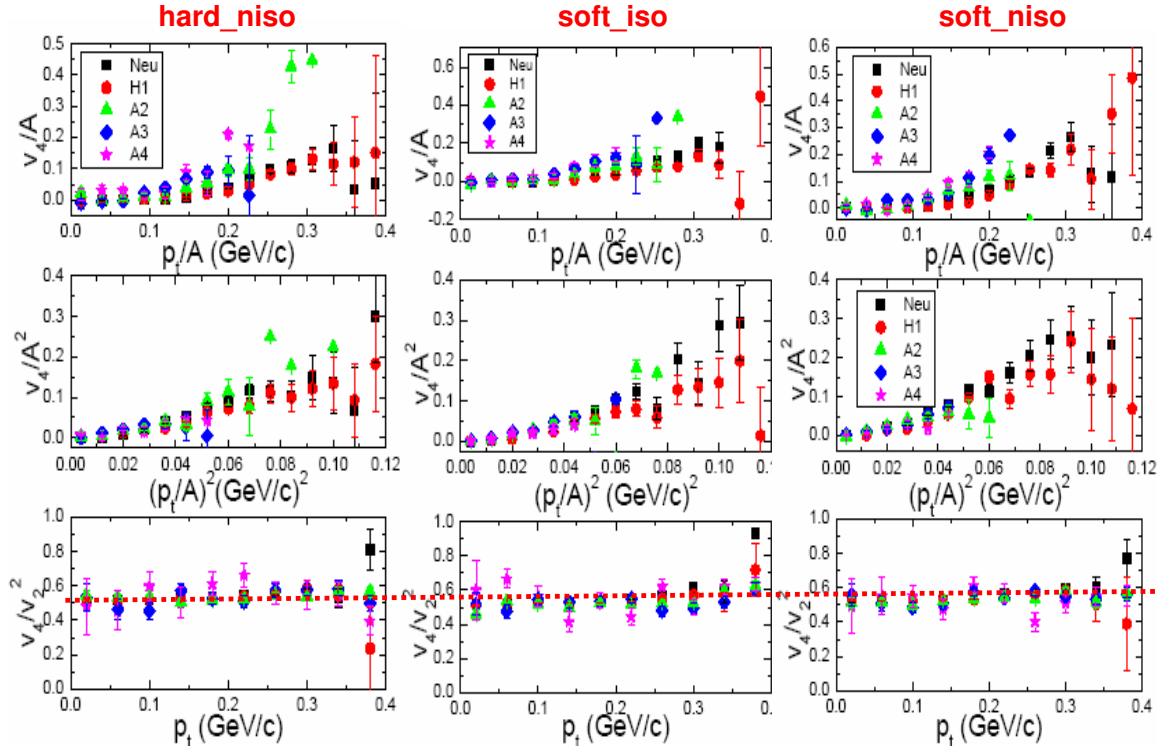


Figure 3. The upper panels: v_4/A as a function of p_t/A for different particles, namely, neutrons (squares), protons (circles), fragments of $A = 2$ (triangles), $A = 3$ (diamonds) and $A = 4$ (stars) in three different calculation conditions. The middle panels: v_4/A^2 as a function of $(p_t/A)^2$. The lower panels: the ratios of v_4/v_2^2 for different particles vs p_t . Three simulations were done in this figure as Fig. 2.

anisotropy in the intermediate energy is. In the present work, we explore the behavior of v_4 in the model calculation. Fig. 3 shows the features of v_4 for $^{86}\text{Kr} + ^{124}\text{Sn}$ at 25 MeV/nucleon for IDQMD simulation with `hard_niso`, `soft_iso` and `soft_niso`. Similar to the relationship of v_2/A versus p_t/A , we plot v_4/A as a function of p_t/A (the upper panel). The divergence of the different curves between different particles in v_4/A versus p_t/A indicates no simple scaling of nucleon number for 4-th momentum anisotropy. However, if we plot v_4/A^2 versus $(p_t/A)^2$ (the middle panels), it looks that the points of different particles nearly merge together and it means a certain of scaling holds between two variables. Due to a nearly constant value of v_4/v_2^2 in the studied p_t range (see the bottom panels in Fig. 3) together with the number-of-nucleon scaling behavior of v_2/A vs p_t/A , v_4/A^2 should scale with $(p_t/A)^2$, as shown in the middle panels of Fig. 3. Interestingly, the constant value of v_4/v_2^2 does not depend on the EOS and isospin dependent term, which may indicate this constant value is robust for intermediate energy heavy ion collision.

The RHIC experimental data demonstrated a scaling relationship between 2-nd flow (v_2) and n-th flow (v_n), namely $v_n(p_t) \sim v_2^{n/2}(p_t)$ [38]. It has been shown [39, 40] that such scaling relation follows from a naive quark coalescence model [14] that only allows quarks with equal momentum to form a hadron. Denoting the meson anisotropic flows by $v_{n,M}(p_t)$ and baryon anisotropic flows by $v_{n,B}(p_t)$, it was found that $v_{4,M}(p_t) = (1/4)v_{2,M}^2(p_t)$ for mesons and $v_{4,B}(p_t) = (1/3)v_{2,B}^2(p_t)$ for baryons if quarks have no higher-order anisotropic flows. Since mesons dominate the yield of charged particles in RHIC data, the smaller scaling factor of 1/4 than the empirical value of about 1 indicates that higher-order quark anisotropic flows cannot be neglected. Including the latter contribution, one can show that

$$\frac{v_{4,M}}{v_{2,M}^2} \approx \frac{1}{4} + \frac{1}{2} \frac{v_{4,q}}{v_{2,q}^2}, \quad \frac{v_{4,B}}{v_{2,B}^2} \approx \frac{1}{3} + \frac{1}{3} \frac{v_{4,q}}{v_{2,q}^2}, \quad (7)$$

where $v_{n,q}$ denotes the quark anisotropic flows. The meson anisotropic flows thus satisfy the scaling relations if the quark anisotropic flows also satisfy such relations. One can go one step further and assume that the observed scaling of the hadronic v_2 actually results from a similar scaling occurring at the partonic level. In this case, if one assumes [39, 40] that the scaling relation for the partons is as follows:

$$v_4^q = (v_2^q)^2, \quad (8)$$

and then hadronic ratio v_4/v_2^2 then equals $1/4 + 1/2 = 3/4$ for mesons and $1/3 + 1/3 = 2/3$ for baryons, respectively.

If we assume the scaling laws of mesons (NCQ=2) and baryons (NCQ=3) (Eq. 7) are also valid for A = 2 and 3 nuclear clusters, respectively, then v_4/v_2^2 for A = 2 and 3 clusters indeed give the same value of 1/2 as nucleons, as shown in Fig. 3(c). Coincidentally the predicted value of the ratio of v_4/v_2^2 for hadrons is also 1/2 if the matter produced in ultra-relativistic heavy ion collisions reaches to thermal equilibrium and its subsequent evolution follows the laws of ideal fluid dynamics [41]. It is interesting to note the same ratio was predicted in two different models at very different energies, which is of course worth to be further investigated in near future.

5. Summary

In summary, we have investigated the behavior of anisotropic flows, namely v_1 , v_2 and v_4 , for light nuclear fragments produced by $^{40}\text{Ca} + ^{40}\text{Ca}$, $^{86}\text{Kr} + ^{58}\text{Ni}$ and $^{86}\text{Kr} + ^{124}\text{Sn}$ at 25 MeV/nucleon for peripheral collisions in the framework of quantum molecular dynamics model. v_1 shows a negative slope versus rapidity, indicating the attractive mean field plays a dominant role in directed flow. Both v_2 and v_4 generally show positive values and increase with p_t . The positive v_2 illustrates that the in-plane emission is preferential. By the scaling of the number-of-nucleons, both v_1/A versus rapidity and v_2/A versus p_t/A for light nuclear fragments approximately collapse on the similar curve, respectively, which means that there exists directed flow and elliptic flow scalings on the number-of-nucleon. Nucleon-number scaling originates from nucleonic coalescence. For 4-th momentum anisotropy v_4 , it seems to be scaled by v_2^2 , and v_4/v_2^2 is a constant, i.e. $1/2$, for light nuclear fragments. Comparing our above predictions with intermediate energy HIC data for the flow scalings which is presented in this work is expected to shed light on nucleonic collectivity and its rich features.

6. Acknowledgements

This work was supported in part by the Shanghai Development Foundation for Science and Technology under Grant Numbers 05XD14021 and 06JC14082, the National Natural Science Foundation of China under Grant No 10535010, 10328259 and 10135030.

REFERENCES

1. J. Ollitrault, Phys. Rev. D 46 (1992) 229.
2. S. Voloshin, Y. Zhang, Z. Phys. C 70 (1996) 665.
3. H. Sorge, Phys. Lett. B 402 (1997) 251; Phys. Rev. Lett. 78 (1997) 2309.
4. P. Danielewicz, R. A. Lacey, P. B. Gossiaux et al., Phys. Rev. Lett. 81 (1998) 2438.
5. B. Zhang, M. Gyulassy, and C. M. Ko, Phys. Lett. B 455(1999) 45.
6. D. Teaney and E. V. Shuryak, Phys. Rev. Lett. 83 (1999) 4951.
7. P. F. Kolb, J. Sollfrank, and U. Heinz, Phys. Rev. C 62 (2000) 054909.
8. Y. Zheng, C. M. Ko, B. A. Li, and B. Zhang, Phys. Rev. Lett. 83 (1999) 2534.
9. D. Perlmutter and C. Gale, Phys. Rev. C 65 (2002) 064611.
10. Y. G. Ma et al., Phys. Rev. C 48 (1993) R1492; Z. Phys. A 344 (1993) 469; Phys. Rev. C 51 (1995) 1029; Phys. Rev. C 51 (1995) 3256.
11. J. Lukasik et al. (INDRA-ALDAIN Collaboration), Phys. Lett. B 608 (2004) 223.
12. STAR Collaboration, Nucl. Phys. A 757 (2005) 102; PHENIX Collaboration, Nucl. Phys. A 757 (2005) 184.
13. Zi-Wei Lin and C. M. Ko, Phys. Rev. Lett. 89 (2002) 202302; V. Greco, C. M. Ko, and P. Lévai, Phys. Rev. C 68 (2003) 034904 .
14. D. Molnár and S. A. Voloshin, Phys. Rev. Lett. 91 (2003) 092301.
15. R. J. Fries, B. Müller, C. Nonaka, and S. A. Bass, Phys. Rev. Lett. 90 (2003) 202303; Phys. Rev. C 68 (2003) 044902.
16. R. C. Hwa and C. B. Yang, Phys. Rev. C 66 (2002) 025205; Phys. Rev. C 70 (2004) 024904.

17. J. H. Chen, Y. G. Ma, G. L. Ma et al., arXiv:nucl-th/0504055, accepted by Phys. Rev. C.
18. Y. G. Ma, nucl-ex/0609020, SQM2005 Proceeding, to appear on J. Phys. G.
19. T. C. Awes, G. Poggi, C. K. Gelbke et al., Phys. Rev. C 24 (1981) 89.
20. A. Z. Mekjian, Phys. Rev. C 17 (1978) 1051; Phys. Rev. Lett. 38 (1977) 640; Phys. Lett. 89B (1980) 177 .
21. H. Sato and K. Yazaki, Phys. Lett. 98B (1981) 153.
22. W. J. Llope, S. E. Pratt, N. Frazier et al., Phys. Rev. C 52 (1995) 002004.
23. K. Hagel, R. Wada, J. Cibor et al., Phys. Rev. C 62 (2000) 034607.
24. M. J. Huang, R. C. Lemmon, F. Daffin, et al., Phys. Rev. Lett. 77 (1996) 3739 .
25. G. J. Kunde, W. C. Hsi, W. D. Kunze et al., Phys. Rev. Lett. 74 (1995) 38.
26. J. Aichelin, Phys. Rep. 202 (1991) 233.
27. Y. B. Wei, Y. G. Ma, W. Q. Shen et al., Phys. Lett. B 586 (2004) 225; J. Phys. G 30 (2004) 2019.
28. Y. G. Ma, Y. B. Wei, W. Q. Shen et al., Phys. Rev. C 73 (2006) 014604.
29. Y. G. Ma and W.Q. Shen, Phys. Rev. C 51 (1995) 710.
30. T. Z. Yan, Y. G. Ma, X. Z. Cai et al., Phys. Lett. B 638 (2006) 50.
31. Y. G. Ma, AIP Conference Proceeding of "The 6th China-Japan Joint Nuclear Physics Symposium", edited by Y. G. Ma and A. Ozawa.
32. For a review, see W. Reisdorf and H. G. Ritter, Annu. Rev. Nucl. Part. Sci. 47 (1997) 663.
33. J. P. Sullivan and J. Péter, Nucl. Phys. A 540 (1992) 275.
34. W. Q. Shen, J. Péter, G. Bizard et al., Nucl. Phys. A 551 (1993) 333.
35. R. Lacey, A. Elmaani, J. Lauret et al., Phys. Rev. Lett. 70 (1993) 1224.
36. Z. Y. He, J.C. Angelique, A. Auger et al., Nucl. Phys. A 598 (1996) 248.
37. J. Adams et al. [STAR Collaboration], Phys. Rev. C 72 (2005) 014904.
38. J. Adams et al. [STAR Collaboration], Phys. Rev. Lett. 92 (2004) 062301.
39. P. F. Kolb, L. W. Chen, V. Greco, C. M. Ko, Phys. Rev. C69 (2004) 051901.
40. L. W. Chen, C. M. Ko, Zi-Wei Lin, Phys. Rev. C69 (2004) 031901(R).
41. N. Borghini and J-Y. Ollitrault, nucl-th/0506045.